Bulletin of Mathematical Biology (2010) 72: 1069–1091
DOI 10.1007/s11538-009-9482-y

ORIGINAL ARTICLE

Response of Tumor Spheroids to Radiation: Modeling and Parameter Estimation

A. Bertuzzi[a,*], C. Bruni[b], A. Fasano[c], A. Gandolfi[a], F. Papa[b], C. Sinisgalli[a]

[a] *Istituto di Analisi dei Sistemi ed Informatica "A. Ruberti", CNR, Viale Manzoni 30, 00185 Rome, Italy*
[b] *Dipartimento di Informatica e Sistemistica "A. Ruberti", Sapienza Università di Roma, Via Ariosto 25, 00185 Rome, Italy*
[c] *Dipartimento di Matematica "U. Dini", Università di Firenze, Viale Morgagni 67/A, 50134 Florence, Italy*

Received: 28 July 2009 / Accepted: 3 November 2009 / Published online: 14 November 2009

Abstract We propose a spatially distributed continuous model for the spheroid response to radiation, in which the oxygen distribution is represented by means of a diffusion-consumption equation and the radiosensitivity parameters depend on the oxygen concentration. The induction of lethally damaged cells by a pulse of radiation, their death, and the degradation of dead cells are included. The compartments of lethally damaged cells and of dead cells are subdivided into different subcompartments to simulate the delays that occur in cell death and cell degradation, with a gain in model flexibility. It is shown that, for a single irradiation and under the hypothesis of a sufficiently small spheroid radius, the model can be reformulated as a linear stationary ordinary differential equation system. For this system, the parameter identifiability has been investigated, showing that the set of unknown parameters can be univocally identified by exploiting the response of the model to at least two different radiation doses. Experimental data from spheroids originated from different cell lines are used to identify the unknown parameters and to test the predictive capability of the model with satisfactory results.

Keywords Tumor spheroids · Radiotherapy · Linear quadratic model · Parameter identification

1. Introduction

Multicellular tumor spheroids growing in vitro have been extensively investigated as experimental models of avascular tumours (Mueller-Klieser, 1987; Sutherland, 1988).

*Corresponding author.
E-mail addresses: bertuzzi@iasi.cnr.it (A. Bertuzzi), bruni@dis.uniroma1.it (C. Bruni), fasano@math.unifi.it (A. Fasano), gandolfi@iasi.cnr.it (A. Gandolfi), papa@dis.uniroma1.it (F. Papa), sinisgalli@iasi.cnr.it (C. Sinisgalli).

The fraction of proliferating cells decreases during the growth of the spheroid while a population of quiescent cells arises, and when the cells become deprived of oxygen and nutrients, and/or metabolic waste accumulates, cell death occurs. In an advanced stage of growth, the spheroid shows an outer viable rim, whose thickness ranges from about 100 to 250 μm, surrounding a necrotic core. Because of the degradation of dead cells in the necrotic core and the loss of waste materials, the spheroid growth eventually saturates with a final diameter of 1–3 mm.

Since the spheroid reproduces important aspects of tumors, such as the presence of oxygen gradients and of subpopulations of quiescent cells, the multicellular spheroids have been used as a valuable experimental models to study the response of solid tumors to drugs and radiation. The in vivo response of cancer cells to treatment may, in fact, be simulated in spheroids more closely than in conventional monolayer cultures. This aspect has originated a large amount of investigations, using ionizing radiations, high LET radiations, radiosensitizing drugs, and cytotoxic drugs (see Mueller-Klieser, 1987 for a review).

Many mathematical models have been proposed to describe the growth of the untreated spheroid by either a continuum or a discrete approach (Araujo and McElwain, 2004). Only few models, however, have been devoted to represent the spheroid response to radiation. Using a 3D cellular automata model, Düchting et al. (1992, 1995) simulated the radiation response of tumor spheroids, including the cycle structure for the tumor cells and the linear-quadratic (LQ) dose-response relationship (Thames, 1985). In that model, the rate of cell division was assumed to decrease with the distance from the external boundary. In Wein et al. (2000), the authors again used the LQ model and since the radiosensitivity of cells is known to decrease as the oxygen concentration decreases, the radiosensitivity parameters were assumed to depend on the radial distance from the spheroid boundary according to a given law. Using several approximations to reduce the mathematical description to an ordinary differential equations (ODE) model, the authors investigated the fractionated irradiation and the possible optimization of the scheduling. By means of a discrete model, Zacharaki et al. (2004) simulated the radiation response of tumor spheroids, including the cell cycle structure and the different radiosensitivities of cells in the different cell cycle phases. Even in this work, the oxygen distribution was not considered and the hypoxic, less sensitive cells were assumed to be located beyond a certain distance from the external boundary.

In the present paper, we propose a spatially distributed (PDE) continuous model for the spheroid response to impulsive irradiation. The oxygen distribution is represented by means of a diffusion-consumption equation and the radiosensitivity parameters of the LQ model depend on the oxygen concentration. As in a previous model of the response to radiation of tumor cords (Bertuzzi et al., 2008), we include the induction of lethally damaged cells after the radiation pulse, cell death, and the degradation of dead cells. Moreover, for a more accurate description of the process leading to cell death and of the fate of dead cells, the compartments of lethally damaged cells and of dead cells are subdivided into subcompartments, so simulating a delayed cell death and cell degradation. This choice resulted in an improvement of model fitting capability. It is also shown that, for a single irradiation and under the hypothesis of a sufficiently small spheroid radius, the PDE model is equivalent to a linear stationary ODE system, provided that the initial condition is derived from the oxygen distribution at the time of irradiation. The parameter identifiability property of this system has been investigated,

showing that the set of unknown parameters can be univocally identified by exploiting the response of the model to at least two different doses of radiation. Experimental data of spheroids initiated from different cell lines (Jostes et al., 1985; Rofstad et al., 1986; Evans et al., 1986) were used to identify the unknown parameters and to test the predictive capability of the model with satisfactory results.

2. Model of the spheroid response to radiation

Radiation produces a variety of lesions in the cell (Sachs et al., 1997). These lesions induce a lethal damage in a fraction of cells (clonogenically dead cells) that lose the capability of unlimited proliferation and will die, after some delay, at a subsequent time. Thus, after irradiation, the living tumor cell population will be composed by a subpopulation of intact, viable cells and a subpopulation of live but lethally damaged, clonogenically dead cells. The death of lethally damaged cells may occur by premitotic apoptosis or after one or more cell divisions (postmitotic apoptosis) (Shinomiya, 2001).

The main pathways of lethal damage production are the direct action of radiation that produces unrepairable damages, and the binary misrepair of double-strand breaks (DSB) of DNA. The kinetics of the repair/misrepair process (Hlatky et al., 1994; Bertuzzi et al., 2008) is here disregarded because in this paper we are interested to the response to treatments in which impulsive irradiations are delivered with intervals much larger than the time constant of this process (of the order of one hour or less). Both the direct action and the effect of binary misrepair will then be considered as instantaneous and described by the LQ dose-response relationship:

$$S = \exp\left[-\alpha d - \beta d^2\right], \tag{1}$$

where S is the surviving fraction of cells after the irradiation, d is the dose, and α and β are the radiosensitivity parameters related to the direct action of radiation and, respectively, to the binary misrepair of DSBs.

Although quiescent cells have been evidenced in tumor spheroids (Freyer and Sutherland, 1985, 1986), we assume for simplicity that all viable cells proliferate with the same rate. In the spheroid, we will distinguish viable cells, lethally damaged cells, and dead cells. Under the continuum hypothesis, we write the model equations in terms of the volume fractions locally occupied by these components. The spheroid is modeled as a sphere of radius R and r denotes the radial distance from the center. Therefore, all the model variables are functions of r and t.

The main assumptions of the model are summarized as follows. (i) The velocity of the cellular components is radially directed and is the same for both live and dead cells. This common velocity is denoted as $u(r, t)$. (ii) All viable cells proliferate with a common constant proliferation rate χ. (iii) Cells die with a constant rate when the oxygen concentration $\sigma(r, t)$ is smaller than a critical value σ_N. (iv) Only impulsive irradiations will be considered, assuming the model (1) with α and β increasing functions of σ. (v) Lethally damaged cells are allowed to progress across the cell cycle and may divide until they die. The death of these cells is assumed to occur after a distributed delay modeled as the passage through a chain of n equal subcompartments having Poisson exit. (vi) Dead cells are degraded to a fluid waste after a delay with gamma distribution still modeled by n equal

subcompartments. (vii) The total volume fraction of cells, denoted by $\nu^\star$, is constant in space and time.

Concerning the assumptions (v) and (vi), we note that a delay between cell exposition to a cytotoxic agent and cell death has been evidenced both after radiation and drug treatment (Montalenti et al., 1998; Sena et al., 1999). Similarly, a time gap between cell death and cell degradation is documented in the literature (Darzynkiewicz et al., 1997). Distributed delays have been included in models of chemotherapy (Bertuzzi et al., 2003; Simeoni et al., 2004; Ubezio and Cameron, 2008) and antiangiogenic therapy (d'Onofrio, 2007). Assumption (vii) amounts to say that live and dead cells possess a uniform spatial arrangement, which is quickly recovered after any perturbation caused by cell proliferation and degradation of dead cells. Here, we have adopted the approximation of an instantaneous removal of the waste material from the neighborhood of a degrading cell. This approach has been widely used in the literature (Araujo and McElwain, 2004) to avoid the complication of describing the flow of the interstitial fluid. Although no physical justification has been provided, we keep this simplification in view of the already high level of complexity of the problem we are considering.

Assuming that all the components have equal mass density, the mass balance yields the following conservation equations for the volume fractions:

$$
\begin{aligned}
\frac{\partial \nu}{\partial t} + \frac{1}{r^2}\frac{\partial}{\partial r}\left(r^2 u \nu\right) &= \chi \nu - \mu(\sigma)\nu,\\
\frac{\partial \nu_{D_1}}{\partial t} + \frac{1}{r^2}\frac{\partial}{\partial r}\left(r^2 u \nu_{D_1}\right) &= \chi_D \nu_{D_1} - \mu_D \nu_{D_1} - \mu(\sigma)\nu_{D_1},\\
\frac{\partial \nu_{D_2}}{\partial t} + \frac{1}{r^2}\frac{\partial}{\partial r}\left(r^2 u \nu_{D_2}\right) &= \chi_D \nu_{D_2} - \mu_D \nu_{D_2} + \mu_D \nu_{D_1} - \mu(\sigma)\nu_{D_2},\\
&\vdots\\
\frac{\partial \nu_{D_n}}{\partial t} + \frac{1}{r^2}\frac{\partial}{\partial r}\left(r^2 u \nu_{D_n}\right) &= \chi_D \nu_{D_n} - \mu_D \nu_{D_n} + \mu_D \nu_{D_{n-1}} - \mu(\sigma)\nu_{D_n},\\
\frac{\partial \nu_{N_1}}{\partial t} + \frac{1}{r^2}\frac{\partial}{\partial r}\left(r^2 u \nu_{N_1}\right) &= \mu(\sigma)\left(\nu + \sum_{i=1}^{n} \nu_{D_i}\right) + \mu_D \nu_{D_n} - \mu_N \nu_{N_1},\\
\frac{\partial \nu_{N_2}}{\partial t} + \frac{1}{r^2}\frac{\partial}{\partial r}\left(r^2 u \nu_{N_2}\right) &= \mu_N \nu_{N_1} - \mu_N \nu_{N_2},\\
&\vdots\\
\frac{\partial \nu_{N_n}}{\partial t} + \frac{1}{r^2}\frac{\partial}{\partial r}\left(r^2 u \nu_{N_n}\right) &= \mu_N \nu_{N_{n-1}} - \mu_N \nu_{N_n},
\end{aligned}
\tag{2}
$$

where $\nu(r,t)$ denotes the local volume fraction of viable cells, $\nu_{D_i}(r,t)$, $i = 1,\ldots,n$, is the local volume fraction of the cells in the ith subcompartment of lethally damaged cells and $\nu_{N_i}(r,t)$, $i = 1,\ldots,n$, is the local volume fraction of the cells in the ith subcompartment of dead cells; see Fig. 1. The proliferation rate of lethally damaged cells is denoted by χ_D, while μ_D and μ_N are the exit rates from the subcompartments of lethally damaged and, respectively, dead cells. Since all the lethally damaged cells are committed to death,

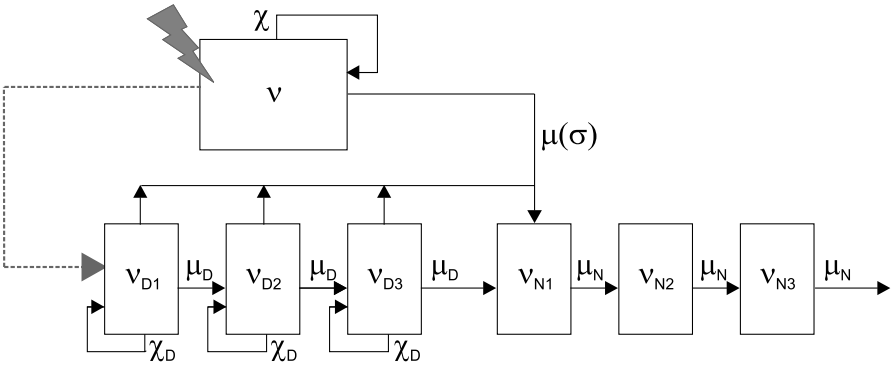

Fig. 1 Block diagram of the model ($n = 3$). The dashed arrow represents the action of radiation.

we must assume $\mu_D > \chi_D$. According to Assumption (iii), the oxygen-dependent death rate $\mu(\sigma)$ has the following form:

$$\mu(\sigma) = \begin{cases} \bar{\mu}, & \sigma < \sigma_N, \\ 0, & \sigma \geq \sigma_N. \end{cases} \tag{3}$$

In view of this choice, if $\bar{\mu} \gg \chi$, a sharp transition from the region of live cells to an almost purely necrotic core is achieved.

Since from Assumption (vii) the sum $\nu + \sum(\nu_{D_i} + \nu_{N_i}) = \nu^\star$ is constant, by summing up all equations in (2), the velocity field $u(r,t)$ is found to satisfy the equation

$$\nu^\star \frac{1}{r^2}\frac{\partial}{\partial r}\big(r^2 u\big) = \chi\nu - \mu_N \nu_{N_n}, \quad u(0,t) = 0. \tag{4}$$

For the evolution of the spheroid radius, we have

$$\dot{R}(t) = u\big(R(t),t\big), \qquad R(0) = R_0. \tag{5}$$

According to Assumption (iv), the direct action of radiation and the misrepair of the DSBs will be represented by suitable initial conditions. We assume that before irradiation all live cells are viable. If a sequence of impulsive irradiations is given with dose d_i at time t_i, $i = 1, 2, \ldots$, with $t_1 = 0$, we have the following initial conditions for Eqs. (2):

$$\begin{aligned} \nu\big(r,t_i^+\big) &= \exp\big[-\alpha\big(\sigma(r,t_i)\big)d_i - \beta\big(\sigma(r,t_i)\big)d_i^2\big]\nu\big(r,t_i^-\big), \\ \nu_{D_1}\big(r,t_i^+\big) &= \big(1 - \exp\big[-\alpha\big(\sigma(r,t_i)\big)d_i - \beta\big(\sigma(r,t_i)\big)d_i^2\big]\big)\nu\big(r,t_i^-\big) + \nu_{D_1}\big(r,t_i^-\big), \\ \nu_{D_j}\big(r,t_i^+\big) &= \nu_{D_j}\big(r,t_i^-\big), \quad j = 2,\ldots,n, \\ \nu_{N_j}\big(r,t_i^+\big) &= \nu_{N_j}\big(r,t_i^-\big), \quad j = 1,\ldots,n. \end{aligned} \tag{6}$$

At $t = 0^-$, we have $\nu(r,0^-) = \nu^0(r)$, $\nu_{D_j}(r,0^-) = 0$, $\nu_{N_j}(r,0^-) = \nu_{N_j}^0(r)$, $j = 2,\ldots,n$. Since $u(0,t) = 0$, no boundary conditions are required for Eqs. (2).

The dependence on the oxygen concentration of the radiosensitivity parameters, α and β, is expressed as

$$\alpha(\sigma) = \alpha_M \psi_\alpha(\sigma), \qquad \beta(\sigma) = \beta_M \psi_\beta^2(\sigma),$$

with

$$\psi_\alpha(\sigma) = \frac{\sigma + \hat{\sigma}/2.5}{\sigma + \hat{\sigma}}, \qquad \psi_\beta(\sigma) = \frac{\sigma + \hat{\sigma}/3}{\sigma + \hat{\sigma}}, \tag{7}$$

where $\hat{\sigma} = 5.776 \times 10^{-3}$ mM (Wouters and Brown, 1997).

As far as the equation for the oxygen concentration σ is concerned, we recall that diffusion is by far the dominant transport mechanism of oxygen in tumor spheroids and that diffusion occurs in a quasi-stationary regime. Assuming for simplicity that the oxygen consumption rate is the same for all live cells, we can write

$$\frac{1}{r^2}\frac{\partial}{\partial r}\left(r^2 \frac{\partial \sigma}{\partial r}\right) = f(\sigma)\left(\nu + \sum_{i=1}^{n} \nu_{D_i}\right), \tag{8}$$

where $f(\sigma)$ is the ratio between the consumption rate per unit volume of live cells and the oxygen diffusion coefficient. For $f(\sigma)$, we have assumed the following form:

$$f(\sigma) = F\frac{\sigma}{K + \sigma}, \tag{9}$$

with F and K suitable positive constants. At the outer boundary $r = R$, i.e., on the spheroid surface, we prescribe the constant oxygen concentration in the medium:

$$\sigma\big(R(t), t\big) = \sigma^\star, \tag{10}$$

with $\sigma^\star > \sigma_N$, whereas at $r = 0$ we prescribe the no-flux condition

$$\left.\frac{\partial \sigma}{\partial r}\right|_{r=0} = 0. \tag{11}$$

It can be shown that in the absence of treatment the above model admits a stationary state with constant radius. In this state, the production of cell volume by proliferation is balanced by the volume loss caused by the elimination of the waste fluids produced by cell degradation in the necrotic region.

3. Single irradiation response: an equivalent ODE model and its identifiability

Let us consider Eq. (8) with (9) and the prescribed boundary conditions (10), (11) in the case in which the right-hand side of (8) is $f(\sigma)\nu^\star$. It may be seen that a spheroid radius R_N will exist such that for $R < R_N$ we have $\sigma(r) > \sigma_N$. The value of R_N depends on $\sigma^\star$, σ_N, $\nu^\star$, and the parameters that characterize the cellular consumption. In standard in vitro conditions with $\sigma^\star = 0.28$ mM, the spheroid radius at which central necrosis starts

to occur was experimentally observed to be 200–300 μm (Freyer, 1988). This range can be taken as a reasonable interval for the R_N values.

We consider now the case of a single irradiation with dose d at $t = 0$ with $R_0 < R_N$. Since it is $\nu(r,t) + \sum \nu_{D_i}(r,t) \le \nu^\star$, $\forall t \ge 0$, it will be $\sigma(r,t) > \sigma_N$ and $\mu(\sigma) = 0$ as far as $R(t) < R_N$. In this condition, we can derive an ODE system for the total volumes of cells in the different cell compartments at time t. We define such volumes as

$$
\begin{aligned}
v_1(t) &= 4\pi \int_0^{R(t)} r^2 \nu(r,t)\, dr, \\
v_{j+1}(t) &= 4\pi \int_0^{R(t)} r^2 \nu_{D_j}(r,t)\, dr, \quad j = 1, \ldots, n, \\
v_{j+n+1}(t) &= 4\pi \int_0^{R(t)} r^2 \nu_{N_j}(r,t)\, dr, \quad j = 1, \ldots, n.
\end{aligned}
$$

By integrating from 0 to $R(t)$ Eqs. (2) multiplied by $4\pi r^2$ and taking (5) into account, it is easy to obtain the following equations:

$$
\begin{aligned}
\dot{v}_1 &= \chi v_1, \\
\dot{v}_2 &= (\chi_D - \mu_D) v_2, \\
\dot{v}_j &= (\chi_D - \mu_D) v_j + \mu_D v_{j-1}, \quad j = 3, \ldots, n+1, \\
\dot{v}_{n+2} &= \mu_D v_{n+1} - \mu_N v_{n+2}, \\
\dot{v}_j &= \mu_N v_{j-1} - \mu_N v_j, \quad j = n+3, \ldots, 2n+1.
\end{aligned}
\tag{12}
$$

If we denote by $w(t)$ the volume of the spheroid at time t, we have the further equation

$$
w(t) = \frac{1}{\nu^\star} \sum_{i=1}^{2n+1} v_i(t), \tag{13}
$$

from which the radius $R(t)$ can be deduced. The equations (12) define a linear, time-invariant dynamical system and (13) is the corresponding linear output equation.

By integrating the initial conditions (6) written for $t_1 = 0$ and multiplied by $4\pi r^2$ from 0 to R_0, and taking into account that $\nu(r, 0^-) = \nu^\star$, we obtain

$$
\begin{aligned}
v_1\big(0^+\big) &= \delta(\alpha_M, \beta_M; R_0, d) v_1\big(0^-\big), \\
v_2\big(0^+\big) &= \big(1 - \delta(\alpha_M, \beta_M; R_0, d)\big) v_1\big(0^-\big), \\
v_j\big(0^+\big) &= 0, \quad j = 3, \ldots, 2n+1,
\end{aligned}
\tag{14}
$$

where

$$
\delta(\alpha_M, \beta_M; R_0, d) = \frac{3}{R_0^3} \int_0^{R_0} r^2 \exp\big[-\alpha_M \psi_\alpha\big(\sigma(r,0)\big) d - \beta_M \psi_\beta^2\big(\sigma(r,0)\big) d^2\big]\, dr, \tag{15}
$$

and $v_1(0^-) = (4/3)\pi R_0^3 \nu^\star = w_0 \nu^\star$, with w_0 denoting the spheroid volume at $t = 0$. Therefore, the solution of the ODE system (12) with the initial conditions (14) gives the same evolution of cell volumes as predicted by the PDE model (2) until $R(t) \le R_N$.

This equivalence cannot be extended to describe the evolution of the spheroid for successive irradiations because the correct re-initialization of (12) at $t = t_i$, $i > 1$, would require the knowledge of $\sigma(r, t_i)$ and $\nu(r, t_i^-)$. However, if $R(t)$ is sufficiently smaller than R_N, the radiosensitivity parameters α and β will be almost independent of σ and can be assumed to be constant. Thus, the effect of treatment might be represented by the following approximate initial conditions:

$$
\begin{aligned}
v_1\big(t_i^+\big) &= \exp\big[-\alpha d_i - \beta d_i^2\big] v_1\big(t_i^-\big), \\
v_2\big(t_i^+\big) &= \big(1 - \exp\big[-\alpha d_i - \beta d_i^2\big]\big) v_1\big(t_i^-\big) + v_2\big(t_i^-\big), \\
v_j\big(t_i^+\big) &= v_j\big(t_i^-\big), \quad j = 3, \ldots, 2n+1,
\end{aligned}
$$

with

$$
\begin{aligned}
v_1\big(0^-\big) &= \nu^\star w_0, \\
v_j\big(0^-\big) &= 0, \qquad j = 2, \ldots, 2n+1.
\end{aligned}
$$

In the following, as suggested by the comparison with experimental data, we chose $n = 3$. It will be shown in the Appendix that for a treatment with a known single dose at $t = 0$, the knowledge of the output $w(t)$ on a finite time interval $[0, \Delta]$ allows the parameters χ, χ_D, μ_D, μ_N in (12), and the quantity δ in (14), to be univocally identified for any $w_0 > 0$, provided that the remaining parameters of the model are assumed known. This means that, given the initial volume and the dose, two different sets of parameters do not exist that produce the same output $w(t)$ on $[0, \Delta]$. It will be also shown that, if two outputs corresponding to sufficiently different doses are available, the parameters α_M and β_M may also be identified. A proof of both these identifiability properties will be given in Appendix.

Based on the above result, it is also possible to state that the identifiability of the ODE model implies the identifiability of the PDE model (2)–(11) in case of a single irradiation if $R(t)$ is smaller than R_N in $[0, \Delta]$, provided that the initial condition of (12) are given by (14) and (15). We remark that the identifiability property is crucial for the well-posedness of the problem of estimating the model parameters from experimental data.

4. Parameter estimation and model validation

We tested the model behavior and estimated the unknown model parameters by using literature data on the untreated growth and on the single-irradiation response of spheroids from four different cell lines (Jostes et al., 1985; Rofstad et al., 1986; Evans et al., 1986) that show a somewhat different response pattern.

Among the parameters of model (2)–(11), the values of σ_N, $\bar{\mu}$, F and K were assumed to be known and were derived from literature data. We set $F = f N_c/(D_O \nu^\star)$, where $f = 1.0 \times 10^{-16}$ mol s^{-1} cell^{-1} is the maximal oxygen consumption rate per cell (Casciari et al., 1992), $N_c = 5.0 \times 10^8$ cells/cm^3 (Freyer and Sutherland, 1985) is the number of

cells per unit volume, $D_O = 1.82 \times 10^{-5}$ cm^2/s (Mueller-Klieser, 1984) is the oxygen diffusion coefficient, and $\nu^\star = 0.6$ (Freyer and Sutherland, 1985). Thus, we have $F = 4.58 \times 10^{-3}$ mol cm^{-5}. For K, we have taken $K = 4.64$ μM (Casciari et al., 1992). We assumed $\sigma_N = 5$ μM, so that the radius R_N is equal to about 280 μm when $\sigma^\star = 0.28$ mM, in agreement with the experimental values of the viable rim at the onset of central necrosis (Freyer and Sutherland, 1986). For $\bar{\mu}$, we have chosen a value of 0.15 h^{-1}, which is large enough to produce an almost instantaneous cell death: for larger values, the model was found to be virtually not sensitive to $\bar{\mu}$.

The remaining parameters, χ, χ_D, μ_D, μ_N, α_M, and β_M, assumed to be dose independent, were estimated from the available measurements of spheroid radius during the unperturbed growth and after single irradiations with different doses. We observe that the identification problem may be tackled in two successive steps: in fact, the model response when the dose is zero only depends on χ and, possibly, μ_N. Therefore, in the first step, we have estimated these parameters by exploiting the data from the unperturbed growth of the spheroid, and successively the remaining parameters from the data of the response to treatment. In some experimental conditions, namely when necrosis is not formed, the zero-dose response does not depend on μ_N and this parameter has been identified from the treatment data.

As it is well known, a Markov-type estimation procedure that accounts for the variances of the different measurements, guarantees good properties for the estimates. However, the variances of the considered experimental data were not always available and, therefore, we adopted the ordinary least-squares approach. Let us denote by θ the p-dimensional vector of the unknown parameters, and by z_{ij} the measured spheroid radius at time t_i when the dose is d_j. The least-squares estimation of θ was performed by minimizing the following index:

$$J(\theta) = \sum_{j=1}^{m} \sum_{i=1}^{n_j} \big(R(t_i, d_j; \theta) - z_{ij}\big)^2, \tag{16}$$

where m is the number of doses, n_j is the number of available measurements for the dose d_j, and $R(t_i, d_j; \theta)$ denotes the model-predicted spheroid radius at time t_i when the dose given at $t = 0$ is d_j. In the first step of our estimation procedure, it is obviously $m = 1$ and $d_1 = 0$. In all cases, the model prediction $R(t_i, d_j; \theta)$ was computed by assuming $R(0) = R_0$, R_0 known and equal to the radius measured at the irradiation time. The minimization of the function (16) was performed by the Levenberg–Marquardt algorithm (free C code available at http://www.ics.forth.gr) taking into account the physical positivity constraint for all the parameters and the constraint $\mu_D > \chi_D$. This algorithm also allows the computation of the covariance matrix of the estimated parameters and, consequently, provides the coefficients of variation (CV) of the estimates. This calculation is based on the linearization method and yields

$$\mathrm{Cov}\big(\hat{\theta}\big) = s^2 \left(\frac{dR}{d\theta}\bigg|_{\hat{\theta}}^{T} \frac{dR}{d\theta}\bigg|_{\hat{\theta}} \right)^{-1},$$

where $\hat{\theta}$ is the vector of the estimated parameters, R is the vector with components $R(t_i, d_j; \theta)$ for all i and j, and s^2 is the estimate of the common variance of the mea-

surements, given by

$$s^2 = \frac{J(\hat{\theta})}{\sum_{j=1}^{m} n_j - p}.$$

Although all the unknown parameters have been shown to be identifiable, in practice, likely because of the small number of data points, the estimation of five parameters from the available data did not give sufficiently reliable results (some of the CVs greater than 70%). Therefore, when μ_N could not be estimated from the zero-dose response, we reduced the number of the unknown parameters by setting $\chi_D = \chi$. This simplifying assumption yielded more satisfactory CV values.

4.1. Spheroid 9L (Jostes et al., 1985)

The first set of data we considered consisted of measurements of the response to radiation of the spheroid 9L originated by rat brain tumor cells. The parameters χ and μ_N were estimated from the untreated growth curve data, and the corresponding fitting is shown in Fig. 2, left panel. The parameter values with the corresponding CVs are reported in Table 1. The spheroid reaches a radius of about 800 μm and shows a trend to saturation. According to our model, the onset of central necrosis should occur at about 5 days.

The other parameters, χ_D, μ_D, α_M, and β_M, were estimated from the data of the spheroids treated with doses of 4 and 8 Gy (Table 1) and the corresponding fitting is shown in

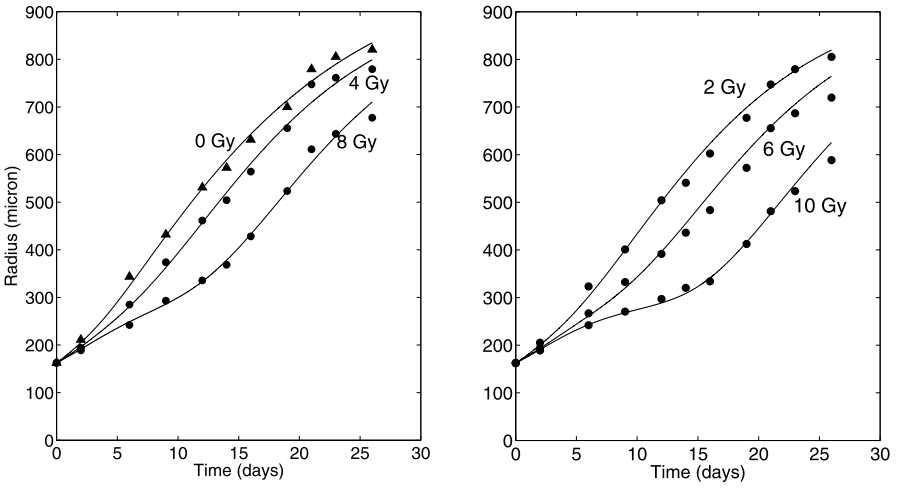

Fig. 2 Growth curves of 9L spheroid: optimal fitting (left panel) and prediction (right panel).

Table 1 Estimated parameters and corresponding CVs for the 9L spheroid

	χ (h^{-1})	μ_N (h^{-1})	χ_D (h^{-1})	μ_D (h^{-1})	α_M (Gy^{-1})	β_M (Gy^{-2})
Estimate	1.4×10^{-2}	3.6×10^{-2}	1.1×10^{-2}	1.9×10^{-2}	0.121	0.026
CV (%)	2.35	25.6	22.5	31.9	38.7	23.6

the left panel of Fig. 2. As already pointed out, at least two different doses are necessary to identify the radiosensitivities α_M and β_M. Even at the largest doses, the data show a continuous, although delayed, increase of spheroid radius. The right panel of Fig. 2 shows the prediction, obtained with the identified model, of the response to three further doses of radiation (namely 2, 6, and 10 Gy). The predictive capacity appears to be quite good: the model correctly reproduces the initial part of the response and the increase of the growth delay with the dose.

4.2. Spheroid GE (Rofstad et al., 1986)

The second set of data consisted of measurements of the response to radiation of the spheroid GE, initiated from human melanoma cells. From the untreated growth curve, the parameter χ was estimated (Table 2) and the corresponding fitting is shown in the left panel of Fig. 3. We observe that, in this case (and in the following), the growth curve of the untreated spheroid made it possible to estimate χ only, because the spheroid did not reach the radius at which the central necrosis develops. After setting $\chi_D = \chi$, the other parameters, μ_D, μ_N, α_M, and β_M, were estimated from the data of the spheroids treated with 2, 4 and 7 Gy (Table 2). The fitting is shown in Fig. 3, left panel. The right panel of Fig. 3 shows the predictions for the doses of 5 and 6 Gy.

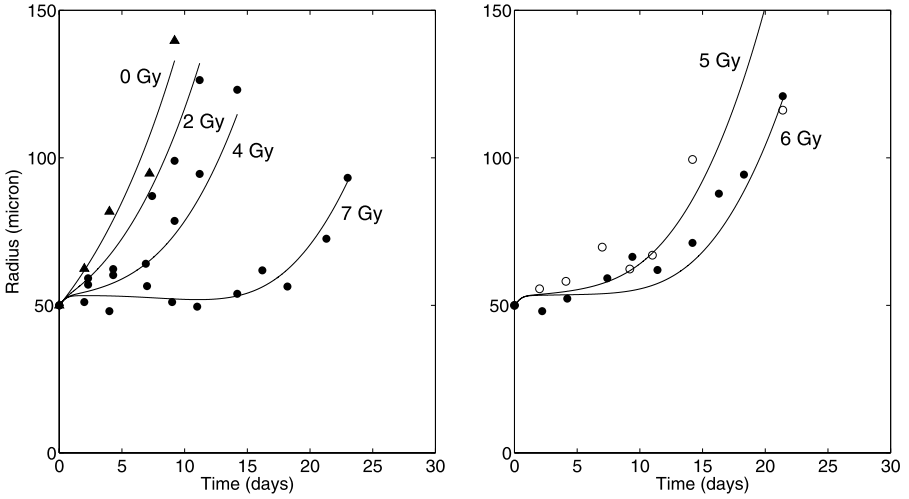

Fig. 3 Growth curves of GE spheroid: optimal fitting (left panel) and prediction (right panel).

Table 2 Estimated parameters and corresponding CVs for the GE spheroid

	$\chi = \chi_D$ (h^{-1})	μ_N (h^{-1})	μ_D (h^{-1})	α_M (Gy^{-1})	β_M (Gy^{-2})
Estimate	1.33×10^{-2}	5.74×10^{-3}	21.7×10^{-2}	0.163	0.094
CV (%)	4.87	46.6	66.9	28.8	9.26

4.3. *Spheroid Lan-1* (Evans et al., 1986)

The response to radiation of the spheroid Lan-1, originated by human neuroblastoma cells, exhibits a very different pattern with respect to the previous cases, showing a regression of the spheroid radius at high radiation doses. The parameter χ was estimated from the untreated growth curve (Table 3) and the corresponding fitting is shown in the left panel of Fig. 4. As in the previous case, the evolution does not reach the radius at which central necrosis develops, so we did not estimate μ_N from the untreated growth curve. The other parameters, μ_D, μ_N, α_M, and β_M, were estimated from the data of spheroids treated with doses of 3, 7, and 12 Gy while χ_D was set equal to χ (Table 3 and Fig. 4, left panel). Figure 4, right panel, shows the predictions for doses of 5 and 10 Gy. The left panel of Fig. 4 also shows (dashed lines) the fitting obtained by setting $n = 1$, i.e., without dividing the lethally damaged and dead cells compartments into subcompartments. The introduction of three subcompartments provides a better fit in the initial part of the response at higher doses. A larger number of subcompartments did not give an appreciable improvement of the fitting.

4.4. *Spheroid NB-100* (Evans et al., 1986)

The response of the spheroid NB-100 (human neuroblastoma cells) is similar to that of the Lan-1 spheroid and again shows a regression of the spheroid following the initial

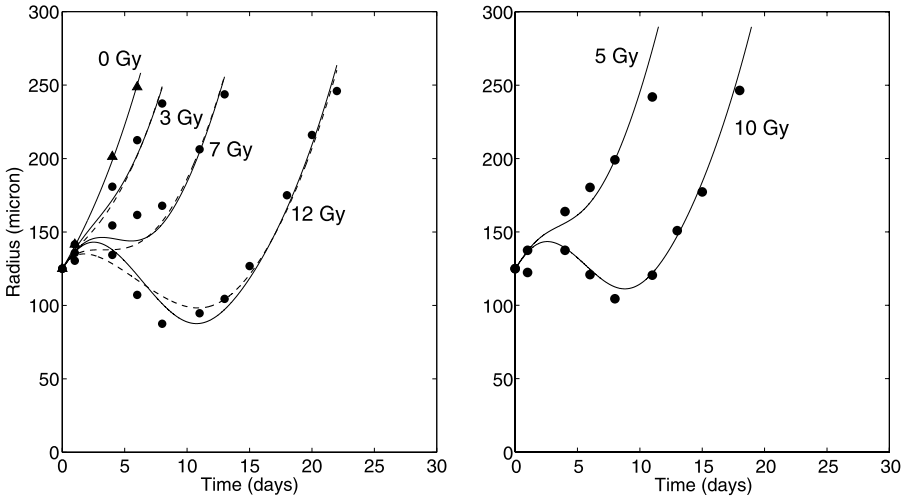

Fig. 4 Growth curves of Lan-1 spheroid: optimal fitting (left panel) and prediction (right panel). Optimal fitting with $n = 1$ (dashed lines).

Table 3 Estimated parameters and corresponding CVs for the Lan-1 spheroid

	$\chi = \chi_D$ (h^{-1})	μ_N (h^{-1})	μ_D (h^{-1})	α_M (Gy^{-1})	β_M (Gy^{-2})
Estimate	1.45×10^{-2}	2.49×10^{-2}	9.27×10^{-2}	0.186	0.023
CV (%)	1.00	23.9	29.4	14.7	10.9

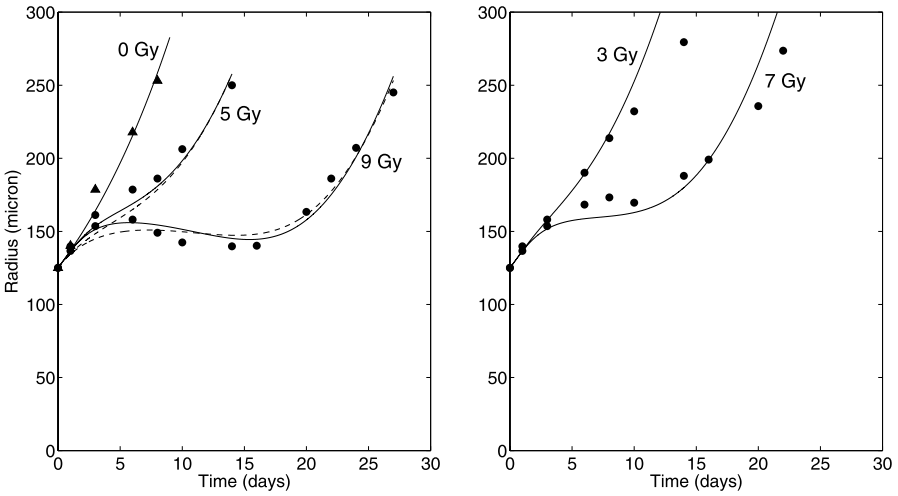

Fig. 5 Growth curves of NB-100 spheroid: optimal fitting (left panel) and prediction (right panel). Optimal fitting with $n = 1$ (dashed lines).

Table 4 Estimated parameters and corresponding CVs for the NB-100 spheroid

	$\chi = \chi_D$ (h^{-1})	μ_N (h^{-1})	μ_D (h^{-1})	α_M (Gy^{-1})	β_M (Gy^{-2})
Estimate	1.13×10^{-2}	7.68×10^{-3}	5.47×10^{-2}	0.072	0.059
CV (%)	3.52	19.3	11.1	57.0	8.5

growth at the highest dose. The parameter χ, estimated from untreated data, is reported in Table 4, and the corresponding fitting is shown in the left panel of Fig. 5. Also in this case, to obtain reliable estimates, we set $\chi_D = \chi$ and the parameters μ_D, μ_N, α_M, and β_M were estimated from the data of spheroids treated with 5 and 9 Gy (see Table 4 and Fig. 5, left panel). The right panel of Fig. 5 shows the predictions for the doses 3 and 7 Gy. Figure 5, left panel, also shows the fitting obtained by setting $n = 1$ (dashed line). Although to a smaller extent than in the case of Lan-1 spheroid, three subcompartments still give a better fit of the initial response at higher doses.

5. Concluding remarks

A model for the response of tumor spheroids to radiation is proposed in this paper. The model takes into account the chain of events that follow the irradiation, namely the production of lethally damaged cells, their death and the degradation of dead cells, and allows to represent the distributed delays among these events. Considering the case of impulsive irradiation, we assumed that lethally damaged cells are instantaneously induced according to the linear quadratic dose-response relationship. The underlying spheroid model assumes that cells die at high rate when the oxygen concentration is below a threshold value, so producing a necrotic core. In case of small spheroids, and of a single irradiation,

the space dependence of variables can be disregarded and the PDE model can be reduced to a linear ODE model. For such a model, a formal study of parameter identifiability has been developed.

The comparison of the model response with four different sets of experimental data gave satisfactory results either in the optimal fitting and in the prediction. Some parameters were estimated with rather large coefficients of variation (μ_N and μ_D in Table 2 and α_M in Table 4), which is generally to be expected when the available measurements are limited in number and precision. However, the main cause of the large CV values of the above parameters was likely the low sensitivity of the model response to their changes, in particular in certain regions of the parameter space.

The model we propose is characterized by $n = 3$ subcompartments of lethally damaged and dead cells. This choice was found to be a reasonable tradeoff between the model complexity and its fitting capability. The choice of $n = 1$ was less suitable to reproduce the rapid shrinkage after the initial growth observed in the spheroids Lan-1 and NB-100 at the highest doses. Moreover, we recall that with $n = 1$ the parameters are not globally identifiable (see the Appendix).

Experimental observations, as for instance the Lan-1 spheroid data, suggest that the model parameters that characterize the behavior of the lethally damaged cells can depend on the radiation dose. To explore this possibility, we tried to estimate the parameters χ_D and μ_D from the Lan-1 data at each single dose by keeping the other parameters at the values given in Table 3. The fitting results are shown in Fig. 6 and the parameters are given in Table 5. The χ_D value was found to decrease as the dose increased, whereas a clear trend was not observed for μ_D. The decrease of χ_D is reasonable, corresponding to a decrease of the proliferative activity of lethally damaged cells with the extent of injury. Correspondingly, we note a marked improvement of the fitting with respect to Fig. 4 especially at 7 and 12 Gy. This result suggests that the model might be improved by

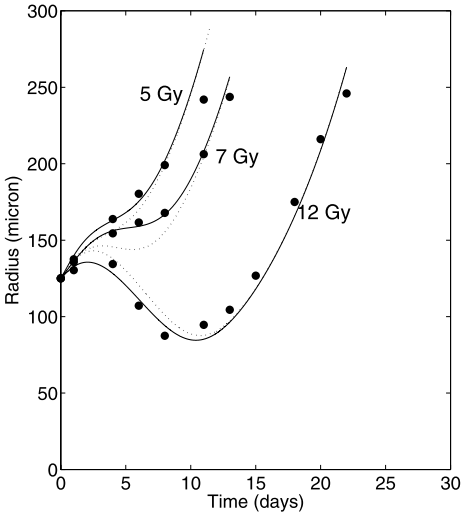

Fig. 6 Growth curve of Lan-1 spheroid: optimal fitting of single-dose responses. For comparison, the dotted lines reproduce the fitting of Fig. 4.

Table 5 Lan-1 spheroid: parameters χ_D and μ_D and corresponding CVs estimated from the response to the indicated doses

Dose (Gy)	χ_D (h^{-1})	μ_D (h^{-1})
5	1.51×10^{-2} (4.53%)	7.29×10^{-2} (43.9%)
7	1.06×10^{-2} (1.95%)	4.91×10^{-2} (10.6%)
12	0.85×10^{-2} (1.70%)	9.14×10^{-2} (20.1%)

introducing a dependence of at least χ_D on the dose. To conserve the predictive capacity of the model, however, a form of this dependence should be assessed and the corresponding parameters identified. This development may be the object of future investigation.

Finally, we observe that from the growth curves of the treated spheroid it was possible to estimate the radiosensitivity parameters α_M and β_M, obtaining values for the α_M/β_M ratio ranging from 1.2 to 8.1, and thus comparable with literature α/β data. A better evaluation of the reliability of the obtained results could be achieved by the comparison of these values with the values determined by the standard procedure involving the surviving fractions at different radiation doses in a colony forming assay (Bristow and Hill, 1998).

Appendix: Parameter identifiability

Single radiation dose

The ODE system (12), the output equation (13), and the initial condition (14) can be rewritten in a compact form as follows:

$$\begin{aligned} \dot{v} &= Av, \\ w &= \frac{1}{v^\star} c^T v, \\ v(0) &= b v^\star w_0, \end{aligned} \tag{A.1}$$

where, in the case of $n = 3$, v is the 7-dimensional state vector with components v_i, and A, c^T and b are 7×7, 1×7 and, respectively, 7×1 matrices. In particular, for the elements of A, we have

$$a_{11} = \chi, \qquad a_{22} = a_{33} = a_{44} = \chi_D - \mu_D, \qquad a_{55} = a_{66} = a_{77} = -\mu_N,$$
$$a_{32} = a_{43} = a_{54} = \mu_D, \qquad a_{65} = a_{76} = \mu_N,$$

all other elements being equal to zero. Moreover, $c_i = 1$, $i = 1, 2, \ldots, 7$, and

$$b_1 = \delta, \qquad b_2 = 1 - \delta, \qquad b_i = 0, \qquad i = 3, 4, \ldots, 7.$$

Denoting by ω the vector of parameters

$$\omega = (\chi \quad \chi_D \quad \mu_D \quad \mu_N \quad \delta)^T$$

ranging in the admissible set Ω, with

$$\Omega = \left\{\omega \in \mathbb{R}^5 : \chi > 0; \mu_D > \chi_D > 0; \mu_N > 0; \delta \in (0,1)\right\},$$

we can write $A = A(\omega)$ and $b = b(\omega)$. With the above notation, we have

$$w(t;\omega) = c^T \exp\big(A(\omega)t\big)b(\omega)w_0, \quad t \geq 0. \tag{A.2}$$

With reference to model (A.1), (A.2), let us recall now the following definitions from the linear systems theory (Kalman et al., 1969).

Definition 1. The parameter vector ω is globally identifiable in Ω if, given ω', $\omega'' \in \Omega$ and $\Delta > 0$, the equality

$$c^T \exp\big(A(\omega')t\big)b(\omega') = c^T \exp\big(A(\omega'')t\big)b(\omega''), \quad t \in [0, \Delta]$$

implies $\omega' = \omega''$.

Definition 2. The pair (A, b) is controllable if

$$\det \mathcal{C} = \det\begin{pmatrix} b & Ab & \cdots & A^6 b \end{pmatrix} \neq 0. \tag{A.3}$$

The pair (A, c^T) is observable if

$$\det \mathcal{O} = \det \begin{pmatrix} c^T \\ c^T A \\ \vdots \\ c^T A^6 \end{pmatrix} \neq 0. \tag{A.4}$$

The triple (c^T, A, b) is controllable and observable if (A.3)–(A.4) hold.

The identifiability of the vector ω will be proved by using the Similarity Transformation Method (Travis and Haddock, 1981). This method is based on the following result:

Theorem. *Let the triples $(c^T, A(\omega'), b(\omega'))$ and $(c^T, A(\omega''), b(\omega''))$ be observable and controllable. Then*

$$c^T \exp\big(A(\omega')t\big)b(\omega') = c^T \exp\big(A(\omega'')t\big)b(\omega''), \quad t \in [0, \Delta] \tag{A.5}$$

if and only if a nonsingular matrix P exists such that

$$\begin{aligned} P A(\omega') P^{-1} &= A(\omega''), \\ c^T P^{-1} &= c^T, \\ P b(\omega') &= b(\omega''). \end{aligned} \tag{A.6}$$

Proof: It is immediate to see that (A.6) implies (A.5) by taking into account the power expansion of the exponential. The inverse implication that requires the controllability and observability properties was proved by Kalman; see Appendix 10.C in Kalman et al. (1969). □

Therefore, we have to prove the following properties.

Proposition 1. *The pair* $(A(\omega), b(\omega))$ *is controllable and the pair* $(A(\omega), c^T)$ *is observable for any* $\omega \in \Omega$.

Proof: By symbolic computation (using MATLAB 7.6), we obtain

$$\det \mathcal{C}(\omega) = \mu_D^{12}\mu_N^3(\chi + \mu_D - \chi_D)^3(\mu_N + \chi)^3\delta(1-\delta)^6.$$

It is immediate to verify that, for $\omega \in \Omega$, each of the factors of the above expression is positive. Similarly, we have

$$\begin{aligned}\det \mathcal{O}(\omega) = &-\mu_N^3\mu_D^3(\chi + \mu_D - \chi_D)^3(\mu_N + \chi)^3 \\ &\times \left(\mu_N^3 + 3\chi_D\mu_N^2 - 3\mu_N\chi_D\mu_D + 3\mu_N\chi_D^2 + \chi_D^3 - 2\chi_D^2\mu_D + \chi_D\mu_D^2\right)^3.\end{aligned}$$

Also, for the above expression, it can be verified that all the factors are positive in Ω. The last factor, in particular, by defining $x = \mu_D/\chi_D > 1$ and $y = \mu_N/\chi_D > 0$, can be written in the following form:

$$\chi_D^9\left[x^2 - (2+3y)x + (1+y)^3\right]^3.$$

It is easy to verify that the second-order polynomial in x in square brackets is always positive for $y > 0$. □

Proposition 2. *Given* $\omega^\star \in \Omega$, *the matrix equations*

$$\begin{aligned} PA(\omega^\star) &= A(\omega)P, \\ c^T &= c^T P, \\ Pb(\omega^\star) &= b(\omega), \end{aligned} \tag{A.7}$$

in the unknown $(P, \omega), \omega \in \Omega$, *have the unique solution* $(I, \omega^\star)$, *where* I *is the identity matrix.*

Proof: The proof, which is rather cumbersome, has been developed by starting with the third equation in (A.7), which allows to express the first column of P in terms of the second column. By exploiting this relation in the first equation, it is possible to verify that P has to be an upper triangular matrix. On the other side, the second equation establishes that the sum of elements of each column of P is equal to 1. Using this information, it follows that P is necessarily the identity matrix and, consequently, that $\omega = \omega^\star$. The detail of the proof is reported in Papa (2009). □

We note that the above procedure, when applied to the case of $n = 1$, shows that the parameters are not globally identifiable while only a local identifiability property holds. In fact, it is possible to see that if the parameter vector $\omega = (\chi\ \chi_D\ \mu_D\ \mu_N\ \delta)^T \in \Omega$ gives rise to a certain output of the model, the same output is also given by $\omega' \in \Omega$ defined by

$$\chi' = \chi, \qquad \chi'_D = \chi_D, \qquad \mu'_D = \chi_D + \mu_N, \qquad \mu'_N = \mu_D - \chi_D, \qquad \delta' = \delta.$$

Multiple radiation doses

The above results allow to state that the model response to a single radiation dose univocally identifies the parameter vector ω. However, as it appears from (15), the parameter δ depends on the pair of parameters α_M and β_M, and these parameters cannot be univocally determined from δ. We show now that α_M and β_M can be univocally identified by exploiting the model responses to at least two sufficiently different radiation doses.

Let us denote by $v^{(1)}$ and $v^{(2)}$ the state responses to the doses d_1 and d_2, respectively, and by $w^{(1)}$ and $w^{(2)}$ the corresponding outputs. In the case of $w^{(1)}(0) = w^{(2)}(0) = w_0$, denoting by

$$\bar{v} = \begin{pmatrix} v^{(1)} \\ v^{(2)} \end{pmatrix}, \qquad \bar{w} = \begin{pmatrix} w^{(1)} \\ w^{(2)} \end{pmatrix}, \qquad \bar{w}_0 = \begin{pmatrix} w_0 \\ w_0 \end{pmatrix},$$

we can write

$$\begin{aligned} \dot{\bar{v}} &= \bar{A}\bar{v}, \\ \bar{w} &= \frac{1}{v^\star} C\bar{v}, \\ \bar{v}(0) &= B v^\star \bar{w}_0, \end{aligned}$$

where $\bar{A}$, C, B are block matrices defined as

$$\bar{A} = \begin{pmatrix} A & 0 \\ 0 & A \end{pmatrix}, \qquad C = \begin{pmatrix} c^T & 0 \\ 0 & c^T \end{pmatrix}, \qquad B = \begin{pmatrix} b^{(1)} & 0 \\ 0 & b^{(2)} \end{pmatrix}$$

with

$$b_1^{(j)} = \delta_j, \qquad b_2^{(j)} = 1 - \delta_j, \qquad b_i^{(j)} = 0, \quad i = 3, 4, \ldots, 7, \ j = 1, 2.$$

Recalling (15), the quantities δ_1 and δ_2 are given by

$$\delta_j = \delta(\alpha_M, \beta_M; R_0, d_j), \quad j = 1, 2.$$

Let $\bar{\omega}$ be the parameter vector

$$\bar{\omega} = (\chi \quad \chi_D \quad \mu_D \quad \mu_N \quad \delta_1 \quad \delta_2)^T$$

ranging in the admissible set $\bar{\Omega}$,

$$\bar{\Omega} = \left\{ \bar{\omega} \in \mathbb{R}^6 : \chi > 0; \mu_D > \chi_D > 0; \mu_N > 0; \delta_1, \delta_2 \in (0, 1) \right\},$$

so that we can write $\bar{A} = \bar{A}(\bar{\omega})$ and $B = B(\bar{\omega})$. With the above notation, we have

$$\bar{w}(t;\bar{\omega}) = C\exp\big(\bar{A}(\bar{\omega})t\big)B(\bar{\omega})\bar{w}_0, \quad t \geq 0.$$

In the present case, the properties of controllability and observability are defined as follows:

Definition 3. The pair $(\bar{A}, B)$ is controllable if the matrix

$$\mathcal{C} = \begin{pmatrix} B & \bar{A}B & \cdots & \bar{A}^{13}B \end{pmatrix}$$

has full rank. The pair $(\bar{A}, C)$ is observable if the matrix

$$\mathcal{O} = \begin{pmatrix} C \\ C\bar{A} \\ \vdots \\ C\bar{A}^{13} \end{pmatrix}$$

has full rank.

Similarly to the single output case, we can now prove the following result:

Proposition 3. *The pair $(\bar{A}(\bar{\omega}), B(\bar{\omega}))$ is controllable and the pair $(\bar{A}(\bar{\omega}), C)$ is observable for any $\bar{\omega} \in \bar{\Omega}$.*

Proof: It is immediate to verify that the controllability matrix has the following structure:

$$\mathcal{C} = \begin{pmatrix} b^{(1)} & 0 & Ab^{(1)} & 0 & \cdots & A^{13}b^{(1)} & 0 \\ 0 & b^{(2)} & 0 & Ab^{(2)} & \cdots & 0 & A^{13}b^{(2)} \end{pmatrix}.$$

From the above matrix, we can extract the 14×14 minor

$$\mathcal{M} = \begin{pmatrix} (b^{(1)} & Ab^{(1)} & \cdots & A^6b^{(1)}) & & 0 & \\ & 0 & & & (b^{(2)} & Ab^{(2)} & \cdots & A^6b^{(2)}) \end{pmatrix} = \begin{pmatrix} \mathcal{C}^{(1)} & 0 \\ 0 & \mathcal{C}^{(2)} \end{pmatrix}.$$

Since

$$\det \mathcal{M} = \det \mathcal{C}^{(1)} \cdot \det \mathcal{C}^{(2)},$$

in view of Proposition 1 we have $\det \mathcal{M} > 0$. A similar argument can be carried out to verify that the observability matrix has full rank. □

To complete the proof of identifiability of $\bar{\omega}$, we have to prove the following proposition.

Proposition 4. *Given $\bar{\omega}^\star \in \bar{\Omega}$, the matrix equations*

$$\begin{aligned} \bar{P}\,\bar{A}(\bar{\omega}^\star) &= \bar{A}(\bar{\omega})\,\bar{P}, \\ C &= C\,\bar{P}, \\ \bar{P}\,B(\bar{\omega}^\star) &= B(\bar{\omega}), \end{aligned} \tag{A.8}$$

in the unknown $(\bar{P}, \bar{\omega})$, $\bar{\omega} \in \bar{\Omega}$, have the unique solution $(I, \bar{\omega}^\star)$.

Proof: By decomposing the matrix $\bar{P}$ into four 7×7 submatrices

$$\bar{P} = \begin{pmatrix} P_{11} & P_{12} \\ P_{21} & P_{22} \end{pmatrix},$$

the system (A.8) can be decomposed into the four subsystems:

$$\begin{aligned} P_{jj}\,A(\bar{\omega}^\star) &= A(\bar{\omega})\,P_{jj}, \\ c^T &= c^T P_{jj}, \quad j = 1, 2, \\ P_{jj}\,b^{(j)}(\bar{\omega}^\star) &= b^{(j)}(\bar{\omega}), \end{aligned} \tag{A.9}$$

and

$$\begin{aligned} P_{ij}\,A(\bar{\omega}^\star) &= A(\bar{\omega})\,P_{ij}, \\ 0^T &= c^T P_{ij}, \quad i, j = 1, 2;\ i \neq j, \\ P_{ij}\,b^{(j)}(\bar{\omega}^\star) &= 0. \end{aligned} \tag{A.10}$$

Following the same procedure as in the proof of Proposition 2, from the systems (A.9), we deduce that $P_{11} = P_{22} = I$ and $\bar{\omega} = \bar{\omega}^\star$. From the systems (A.10), taking into account that $\bar{\omega} = \bar{\omega}^\star$, we deduce that $P_{12} = P_{21} = 0$ (Papa, 2009). □

To establish the identifiability of α_M and β_M, it is useful to prove the following result.

Lemma. *Let us define the function*

$$\phi(r) = \frac{\psi_\alpha(\sigma_0(r))}{\psi_\beta^2(\sigma_0(r))},$$

where ψ_α and ψ_β are given by (7), and $\sigma_0(r)$ is the solution of Eqs. (8), (9) with the prescribed boundary conditions in which $R = R_0$ and the right-hand side of (8) is $f(\sigma)v^\star$. We have

$$1 < \phi(R_0) \leq \phi(r) \leq \phi(0) < 9/2.5, \quad \text{for } r \in [0, R_0]. \tag{A.11}$$

Proof: First we recall that

$$\phi(R_0) = \frac{\psi_\alpha(\sigma^\star)}{\psi_\beta^2(\sigma^\star)}, \qquad \phi(0) = \frac{\psi_\alpha(\sigma_0(0))}{\psi_\beta^2(\sigma_0(0))}.$$

Since the ratio $\psi_\alpha(\sigma)/\psi_\beta^2(\sigma)$ is decreasing for $\sigma \geq 0$ and $\sigma_0(r)$ is easily seen to be increasing with r, we have that, for $r \in [0, R_0]$, the minimum value of ϕ is $\phi(R_0)$ and its maximum value is $\phi(0)$. Moreover, since $\psi_\alpha(\sigma)/\psi_\beta^2(\sigma)$ is always smaller than $9/2.5$ and greater than 1, we get the upper and lower bounds given by (A.11). □

Finally, we have the following proposition.

Proposition 5. *Let us assume*

$$\frac{d_2}{d_1} > \frac{\phi(0)}{\phi(R_0)}. \tag{A.12}$$

Given a pair (δ_1, δ_2) *with* δ_1 *and* $\delta_2 \in (0, 1)$, *if the system of equations*

$$\delta(\alpha_M, \beta_M; R_0, d_1) = \delta_1,$$

$$\delta(\alpha_M, \beta_M; R_0, d_2) = \delta_2$$

admits a positive solution (α_M, β_M), *this solution is unique*.

Proof: Let us suppose (α'_M, β'_M) and (α_M, β_M) are such that

$$\delta(\alpha'_M, \beta'_M; R_0, d_1) = \delta(\alpha_M, \beta_M; R_0, d_1), \tag{A.13}$$

$$\delta(\alpha'_M, \beta'_M; R_0, d_2) = \delta(\alpha_M, \beta_M; R_0, d_2). \tag{A.14}$$

Taking Eq. (15) into account and using the mean value theorem, (A.13) can be rewritten as

$$\frac{3}{R_0^3}\left(\mathrm{e}^{-\alpha_M \psi_\alpha(\sigma_0(\bar{r}_1))d_1 - \beta_M \psi_\beta^2(\sigma_0(\bar{r}_1))d_1^2} - \mathrm{e}^{-\alpha'_M \psi_\alpha(\sigma_0(\bar{r}_1))d_1 - \beta'_M \psi_\beta^2(\sigma_0(\bar{r}_1))d_1^2}\right) \int_0^{R_0} r^2\, dr = 0,$$

where $\bar{r}_1$ is a suitable number of the interval $[0, R_0]$. From the previous equation, it follows that

$$(\alpha_M - \alpha'_M)\psi_\alpha\big(\sigma_0(\bar{r}_1)\big)d_1 + (\beta_M - \beta'_M)\psi_\beta^2\big(\sigma_0(\bar{r}_1)\big)d_1^2 = 0. \tag{A.15}$$

In a similar way, from (A.14), we obtain

$$(\alpha_M - \alpha'_M)\psi_\alpha\big(\sigma_0(\bar{r}_2)\big)d_2 + (\beta_M - \beta'_M)\psi_\beta^2\big(\sigma_0(\bar{r}_2)\big)d_2^2 = 0. \tag{A.16}$$

The determinant of the system (A.15), (A.16) is

$$d_1 d_2\big[\psi_\alpha\big(\sigma_0(\bar{r}_1)\big)\psi_\beta^2\big(\sigma_0(\bar{r}_2)\big)d_2 - \psi_\alpha\big(\sigma_0(\bar{r}_2)\big)\psi_\beta^2\big(\sigma_0(\bar{r}_1)\big)d_1\big],$$

and it is different from zero if and only if

$$\frac{d_2}{d_1} \neq \frac{\psi_\alpha(\sigma_0(\bar{r}_2))\psi_\beta^2(\sigma_0(\bar{r}_1))}{\psi_\alpha(\sigma_0(\bar{r}_1))\psi_\beta^2(\sigma_0(\bar{r}_2))} = \frac{\phi(\bar{r}_2)}{\phi(\bar{r}_1)}.$$

In view of (A.11), from the hypothesis (A.12), we see that the determinant is different from zero, and consequently the system (A.15), (A.16) admits the unique solution $\alpha_M = \alpha'_M$, $\beta_M = \beta'_M$. □

References

Araujo, R.P., McElwain, D.L.S., 2004. A history of the study of solid tumour growth: the contribution of mathematical modelling. Bull. Math. Biol. 66, 1039–1091.

Bertuzzi, A., d'Onofrio, A., Fasano, A., Gandolfi, A., 2003. Regression and regrowth of tumour cords following single-dose anticancer treatment. Bull. Math. Biol. 65, 903–931.

Bertuzzi, A., Fasano, A., Gandolfi, A., Sinisgalli, C., 2008. Reoxygenation and split-dose response to radiation in a tumour model with Krogh-type vascular geometry. Bull. Math. Biol. 70, 992–1012.

Bristow, R.G., Hill, R.P., 1998. Molecular and cellular basis of radiotherapy. In: Tannock, I.F., Hill, R.P. (Eds.), The Basic Science of Oncology, pp. 295–321. McGraw-Hill, New York.

Casciari, J.J., Sotirchos, S.V., Sutherland, R.M., 1992. Variations in tumor cell growth rates and metabolism with oxygen concentration, glucose concentration, and extracellular pH. J. Cell. Physiol. 151, 386–394.

Darzynkiewicz, Z., Juan, G., Li, X., Gorczyca, W., Murakami, T., Traganos, F., 1997. Cytometry in cell necrobiology: analysis of apoptosis and accidental cell death (necrosis). Cytometry 27, 1–20.

d'Onofrio, A., 2007. Rapidly acting antitumoral antiangiogenic therapies. Phys. Rev. E Stat. Nonlinear Soft Matter Phys. 76, 031920.

Düchting, W., Ulmer, W., Lehrig, R., Ginzberg, T., Dedeleit, E., 1992. Computer simulation and modelling of tumour spheroid growth and their relevance for optimization of fractionated radiotherapy. Strahlenter. Onkol. 168, 354–360.

Düchting, W., Ginzberg, T., Ulmer, W., 1995. Modeling of radiogenic responses induced by fractionated irradiation in malignant and normal tissue. Stem Cells 13, 301–306.

Evans, S.M., Labs, L.M., Yuhas, J.M., 1986. A cellular automaton model for tumour growth in inhomogeneous environment. Int. J. Radiat. Oncol. Biol. Phys. 12, 969–973.

Freyer, J.P., 1988. Role of necrosis in regulating the growth saturation in multicellular spheroids. Cancer Res. 48, 2432–2439.

Freyer, J.P., Sutherland, R.M., 1985. A reduction in the in situ rates of oxygen and glucose consumption of cells in EMT6/Ro spheroids during growth. J. Cell. Physiol. 124, 516–524.

Freyer, J.P., Sutherland, R.M., 1986. Regulation of growth saturation and development of necrosis in EMT6/Ro multicellular spheroids by the glucose and oxygen supply. Cancer Res. 46, 3504–3512.

Hlatky, L.R., Hahnfeldt, P., Sachs, R.K., 1994. Influence of time-dependent stochastic heterogeneity on the radiation response of a cell population. Math. Biosci. 122, 201–220.

Jostes, R.F., Williams, M.E., Barcellos-Hoff, M.H., Hoshino, T., Deen, D.F., 1985. Growth delay in 9L rat brain tumor spheroids after irradiation with single and split doses of X rays. Radiat. Res. 102, 182–189.

Kalman, R.E., Falb, P.L., Arbib, M.A., 1969. Topics in Mathematical System Theory. McGraw-Hill, New York.

Montalenti, F., Sena, G., Cappella, P., Ubezio, P., 1998. Simulating cancer cell kinetics after drug treatment: application to Cisplatin on ovarian carcinoma. Phys. Rev. E 57, 5877–5887.

Mueller-Klieser, W., 1984. Method for the determination of oxygen consumption rates and diffusion coefficients in multicellular spheroids. Biophys. J. 46, 343–348.

Mueller-Klieser, W., 1987. Multicellular spheroids. a review on cellular aggregates in cancer research. J. Cancer Res. Clin. Oncol. 113, 101–122.

Papa, F., 2009. Models of the tumour spheroid response to radiation: identifiability analysis. Technical report N. 9/2009, Dipartimento di Infomatica e Sistemistica, Sapienza University of Rome.

Rofstad, E.K., Wahl, A., Brustad, T., 1986. Radiation response of multicellular spheroids initiated from five human melanoma xenograft lines. relationship to the radioresponsiveness in vivo. Br. J. Radiol. 59, 1023–1029.

Sachs, R.K., Hahnfeld, P., Brenner, D.J., 1997. The link between low-let dose-response relations and the underlying kinetics of damage production/repair/misrepair. Int. J. Radiat. Biol. 72, 351–374.

Sena, G., Onado, C., Cappella, P., Montalenti, F., Ubezio, P., 1999. Measuring the complexity of cell cycle arrest and killing of drugs: kinetics of phase-specific effects induced by taxol. Cytometry 37, 113–124.

Shinomiya, N., 2001. New concepts in radiation-induced apoptosis: 'premitotic apoptosis' and 'postmitotic apoptosis'. J. Cell. Mol. Med. 5, 240–253.

Simeoni, M., Magni, P., Cammia, C., De Nicolao, G., Croci, V., Pesenti, E., Germani, M., Poggesi, I., Rocchetti, M., 2004. Predictive pharmacokinetic-pharmacodynamic modeling of tumor growth kinetics in xenograft models after administration of anticancer agents. Cancer Res. 64, 1094–1101.

Sutherland, R.M., 1988. Cell and environment interactions in tumor microregions: the multicell spheroid model. Science 240, 177–184.

Thames, H.D., 1985. An 'incomplete-repair' model for survival after fractionated and continuous irradiations. Int. J. Radiat. Biol. 47, 319–339.

Travis, C.C., Haddock, G., 1981. On structural identification. Math. Biosci. 56, 157–173.

Ubezio, P., Cameron, D., 2008. Cell killing and resistance in pre-operative breast cancer chemotherapy. BMC Cancer 8, 201.

Wein, M.L., Cohen, E.J., Wu, J.T., 2000. Dynamic optimization of a linear-quadratic model with incomplete repair and volume-dependent sensitivity and repopulation. Int. J. Radiat. Oncol. Biol. Phys. 47, 1073–1083.

Wouters, B.G., Brown, J.M., 1997. Cells at intermediate oxygen levels can be more important than the 'hypoxic fraction' in determining tumor response to fractionated radiotherapy. Radiat. Res. 147, 541–550.

Zacharaki, E.I., Stamakos, G.S., Nikita, K.S., Uzunoglu, N.K., 2004. Simulating growth dynamics and radiation response of avascular tumour spheroids—model validation in the case of an EMT6/Ro multicellular spheroid. Comput. Methods Programs Biomed. 76, 193–206.